ZrO$_2$ thin-film-based sapphire fiber temperature sensor

Jiajun Wang,[1,*] Evan M. Lally,[1] Xiaoping Wang,[2] Jianmin Gong,[1]
Gary Pickrell,[2] and Anbo Wang[1]

[1]Center for Photonics Technology, The Bradley Department of Electrical and Computer Engineering,
Virginia Polytechnic Institute & State University, Blacksburg, Virginia 24061, USA

[2]Department of Material Science, Virginia Polytechnic Institute & State University, Blacksburg, Virginia 24061, USA

*Corresponding author: wangjj@vt.edu

A submicrometer-thick zirconium dioxide film was deposited on the tip of a polished C-plane sapphire fiber to fabricate a temperature sensor that can work to an extended temperature range. Zirconium dioxide was selected as the thin film material to fabricate the temperature sensor because it has relatively close thermal expansion to that of sapphire, but more importantly it does not react appreciably with sapphire up to 1800 °C. In order to study the properties of the deposited thin film, ZrO$_2$ was also deposited on C-plane sapphire substrates and characterized by x-ray diffraction for phase analysis as well as by atomic force microscopy for analysis of surface morphology. Using low-coherence optical interferometry, the fabricated thin-film-based sapphire fiber sensor was tested in the lab up to 1200 °C and calibrated from 200° to 1000 °C. The temperature resolution is determined to be 5.8 °C when using an Ocean Optics USB4000 spectrometer to detect the reflection spectra from the ZrO$_2$ thin-film temperature sensor.   © 2012 Optical Society of America

OCIS codes: 060.2370, 120.6780, 310.1620.

1. Introduction

Single-crystal sapphire fiber sensors were intensively studied recently for applications in which the maximal operating temperature exceeds 1000 °C. Due to sapphire's supreme material properties, such as high melting point (2040 °C), high hardness, and high resistance to chemical corrosion [1], sapphire fiber-based sensors can potentially work up to 2000 °C without significant performance degradation. Compared with silica fiber sensors, the sapphire fiber ones are generally much more difficult to fabricate because of the highly multi-moded nature of the cladding-less sapphire fiber. Dils proposed a sapphire fiber-based optical thermometer using blackbody radiation in early 1980s [2]. Later, spectrum-based sensing methods were studied in search of higher accuracy. Several sensing schemes have been proposed and demonstrated in the past few decades to fabricate temperature sensors, including wafer- [3] and air gap-based [4,5] Fabry-Perot interferometers (FPIs) and fiber Bragg gratings [6]. Most reported spectrum-based sensing schemes rely on sensors that must be individually fabricated and tested, making them less viable for mass production. The sapphire fiber Bragg gratings-based temperature sensor reported in [6] is batch-fabrication ready, but it requires careful control of the modal excitation condition into the sapphire fiber because a single-mode outputting tunable laser was used to interrogate the Bragg gratings. If many modes are excited in the sapphire fiber, the reflection spectrum from the gratings will be smeared such that the performance of the sensor is greatly compromised. Due to the multi-moded nature of sapphire fibers, modal excitation control presents challenges for applications where long sapphire fibers are needed for this approach.

Previously, we have reported the sensor fabrication using a thin-film coating on sapphire fiber tips

to batch-fabricate sensors [7], and this study Ta_2O_5 was used as the thin film material to fabricate sensors that were demonstrated to work up to 1000 °C. In order to mitigate the film cracking that occurred at higher temperatures and thus extend the working temperature range for the thin-film sensors, TiO_2, whose coefficient of thermal expansion (CTE) matches well with that of sapphire, was then selected as the thin-film material to fabricate the sapphire fiber temperature sensors that were demonstrated to work up to 1200 °C. The maximum working temperature of the TiO_2 thin-film sensors is limited because TiO_2 and sapphire (Al_2O_3) react to form another compound, aluminum titanate, above 1200 °C. This new compound has a very different thermal expansion [8] than that of sapphire; thus the TiO_2 thin film cracks quickly above 1200 °C.

From the aforementioned studies, it was learned that an ideal thin-film material not only has to match sapphire in thermal expansion closely enough such that significant thermal stresses do not occur, but it also has to remain as a separate phase when coexisting with sapphire over the entire desired working temperature range. When searching for a new material to fabricate sapphire thin-film sensors that can work to a higher temperature, we used [9] to check the accumulated thermal expansion for all high-temperature material candidates, and [10] was used to cross-check the phase diagram of the material candidates with respect to sapphire. Parallel to the C-plane of sapphire, as the sapphire fiber tip is, the accumulated thermal expansion from 0 °C to 1200 °C is 1.333%; that for the ZrO_2 over the same temperature range is 1.469%. ZrO_2 and sapphire remain as separate phases up to 1800 °C, based on the phase diagram [10]. Since the ZrO_2 not only has a relatively close match of the CTE to that of sapphire but also remains as a separate phase when coexisting with sapphire, the ZrO_2 thin-film sensors may work up to a much higher temperature than what was reported previously for the Ta_2O_5 sensors [7]. The detailed experimental results using ZrO_2 as the thin-film material are discussed in the following sections.

2. Film Deposition

Sapphire fibers of 75 μm diameter (Micro Materials, Inc.) were first polished using diamond films with a grit size from 30 μm down to 0.5 μm. Then, the sapphire fibers were cleaned in an ultrasonic cleaner and rinsed in acetone, isopropanol, and deionized water in a clean room in preparation for the thin-film deposition.

A ZrO_2 thin film was then deposited on the sapphire fibers by electron beam evaporation (E-beam) (Kurt J. Lesker PVD-250) of 99.99% in purity, with the ZrO_2 tablets in a graphite crucible liner (International Advanced Materials). The sapphire fibers were mounted inside the evaporation chamber with their polished tips pointing down toward the source material. A ZrO_2 thin film approximately 650 nm in thickness was deposited on the sapphire fiber tips at a rate of 0.80 nm/s. Next to the polished sapphire fibers, some sapphire wafers (8 mm × 8 mm) of the same crystal orientation (C-plane) were co-deposited for film characterization purposes. In the following sections, details are discussed for the thin-film deposition, characterization, and the temperature sensor calibration.

3. Film Characterization

Since the deposited sapphire fiber samples are very small, sapphire wafer samples from the same deposition run were used to characterize the deposited ZrO_2 thin film. Because the sapphire wafers and sapphire fibers are both C-Plane in crystalline orientation, it is believed that the characterization results are identical for the fiber samples and the wafer samples.

After the thin-film deposition, the fabricated samples were annealed for several cycles, with the maximum annealing temperature gradually increasing from one cycle to the next. For example, the first annealing took place by heating the sample from room temperature to 400 °C and then cooling back to room temperature. The second annealing was up to 600 °C, and the last annealing was up to 1500 °C. After each annealing, the thin film surface was inspected by a microscope (Carl Zeiss Axiovert 25), and the results are shown in Fig. 1.

Figure 1(a) shows the smooth surface the ZrO_2 thin film after annealed up to 400 °C, in comparison to the surface of an epitaxy-polished sapphire wafer. Due to its close thermal expansion to that of the sapphire substrate, the ZrO_2 thin film has a relatively smooth surface even when annealed up to 1200 °C. However, after annealed at 1500 °C, the surface of the ZrO_2
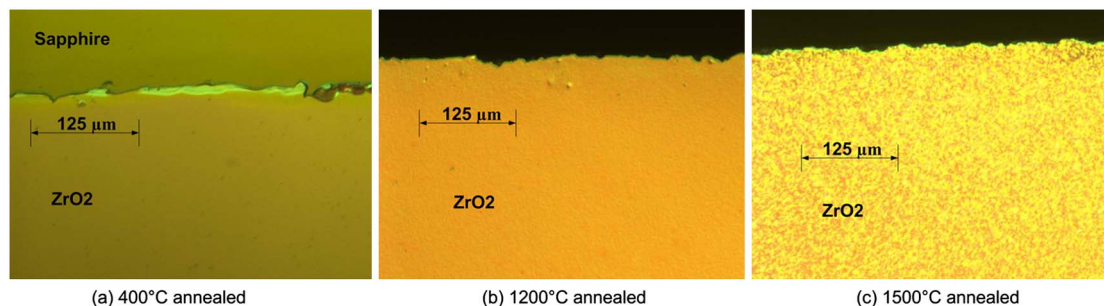

Fig. 1. (Color online) Microscopic images of the ZrO_2 thin film after annealing at different temperatures.

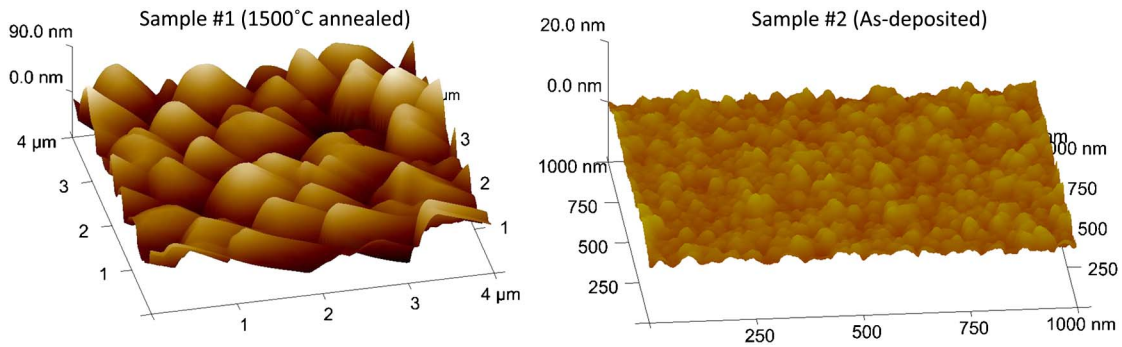(a) 400°C annealed   (b) 1200°C annealed   (c) 1500°C annealed

Fig. 2. (Color online) Surface metrology of the ZrO$_2$ thin film samples.

thin film showed some micro-cracking. In order to further study the surface quality of the ZrO$_2$ thin film after annealing at 1500 °C, Sample #1, which had been annealed by the aforementioned procedures, was compared to Sample #2, which was not annealed at all, to study the changes in the ZrO$_2$ thin film as a result of the high-temperature annealing. The two samples were imaged by an atomic force microscope (AFM, Veeco Nanoscope Dimension 3100); results are presented in Fig. 2. Sample #2, which was not annealed, has a surface roughness of approximately 1.0 nm; Sample #1 has a surface roughness of 20.9 nm after the 1500 °C annealing.

Although the surface roughness degraded a great deal after the 1500 °C annealing, it is still a small fraction of the wavelength of the light used to interrogate the thin film (400 nm–1000 nm). Thus, when a broadband light source was used to interrogate Sample #1, very good interferometric fringes were detected in the reflection spectrum. Figure 3 shows an example of the reflection spectrum of the 1500 °C annealed ZrO$_2$ thin film, as was measured at room temperature.

In order to analyze the changes in the crystal structure of the phases as a result of the high-temperature annealing, x-ray diffraction (XRD, PW1107/PW1140 by Philips) was used to inspect the two samples, whose results are shown in Fig. 4.
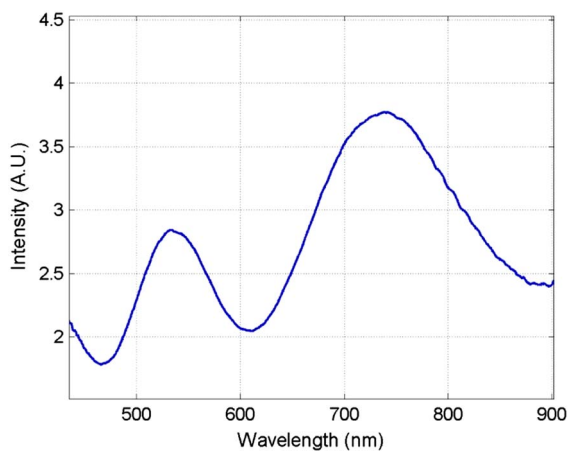
From Fig. 4 it is seen that the most significant peaks correspond to the sapphire substrate in both samples. The peaks corresponding to the alpha alumina in the sapphire substrate occur in the XRD pattern because the x ray has a penetration depth larger than the thickness of the ZrO$_2$ thin film. As is expected, the ZrO$_2$ thin film after deposition did not show any preferred crystal orientation because the E-beam evaporation tends to generate an amorphous film. However, after the 1500 °C annealing, the ZrO$_2$ thin film exhibits peaks associated with the monoclinic zirconia phase. This agrees well with the findings reported by other studies [11–12].

4. Sensor Calibration

A thin film temperature sensor was constructed by fusion splicing [13] of the uncoated end of the sapphire fiber to a multi-mode silica fiber pigtail and connected to the optical interrogation system, as illustrated in Fig. 5.

Light from a tungsten halogen bulb (Ocean Optics, HL-2000) was used to interrogate the thin-film sensor through a 50:50 multi-mode fiber coupler (Gould Optics, 100 μm/140 μm). The light reflected in part from both sides of the deposited ZrO$_2$ thin film generates a periodic interference spectrum $I_{TF}(\lambda)$ (measured with an Ocean Optics USB4000 spectrometer), whose frequency is governed by the optical path difference (OPD) of the ZrO$_2$ thin film. I_{DC} and I_{AC} are the amplitude of the DC and AC components of the interferometric spectrum; $I_h(\lambda)$ is the spectrum of the halogen light source; $I_{sp}(\lambda)$ is the wavelength
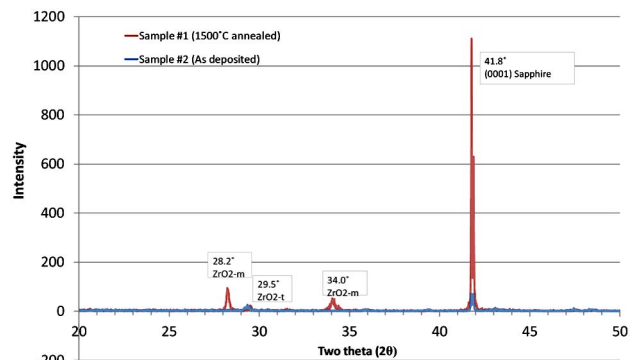

Fig. 3. (Color online) Reflection spectrum of Sample #1 after 1500 °C annealing.

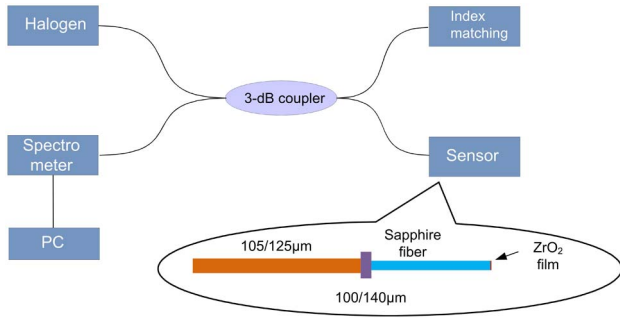Fig. 4. (Color online) XRD results for the sapphire wafer samples.

Fig. 5. (Color online) Optical interrogation system for the ZrO$_2$ thin-film sensors.

dependent transmission coefficient of the entire sapphire to silica fiber link; and $I_s(\lambda)$ is the wavelength-dependent equivalent reflection coefficient from the ZrO$_2$ thin film. Both $I_h(\lambda)$ and $I_{sp}(\lambda)$ can be calibrated in advance. From Fig. 5 it is found that the longer the sapphire fiber is, the weaker the reflection from the thin film, due mainly to the optical loss in the sapphire fiber. On the other hand, as the sapphire fiber becomes shorter, the harder it is to test the sensor at high temperatures because of the degradation of the silica-sapphire splicing point at high temperatures. In experiments, it was found that 15 cm is a good compromise for the length of the sapphire fiber.

Variations in temperature T cause both the film thickness d and refractive index n to change. In turn, this variation in the OPD results in a shift of the wavelength λ_m of the mth peak of the interferometric pattern:

$$
\begin{aligned}
I_{TF}(\lambda) &= I_h(\lambda) \cdot I_{sp}(\lambda) \cdot I_s(\lambda) \\
&= I_h(\lambda) \cdot I_{sp}(\lambda) \\
&\quad \cdot [I_{DC} + I_{AC} \cdot \cos(2\pi OPD/\lambda - \varphi_0)]\lambda_m(T) \\
&= \frac{2n(T)d(T)}{m + \frac{\varphi_0}{2\pi}}, \quad OPD \equiv 2nd.
\end{aligned}
\tag{1}
$$

Temperature-induced shift of a particular peak/valley is determined by the material properties of the ZrO$_2$ thin film, as is pointed out in Eq. (2), where α_d is the linear thermal expansion coefficient of the film, and α_n represents the linear temperature coefficient of the refractive index of the film:

$$
\begin{aligned}
\frac{\Delta\lambda}{\lambda} &\equiv \frac{\lambda_m(T') - \lambda_m(T)}{\lambda_m(T)} = \frac{2n(T')d(T') - 2n(T)d(T)}{2n(T)d(T)} \\
&\approx (1 + \alpha_d \Delta T)(1 + \alpha_n \Delta T) - 1 \\
&= (\alpha_d + \alpha_n)\Delta T + \alpha_d \alpha_n \Delta T^2.
\end{aligned}
\tag{2}
$$

Since the halogen light source that was used to interrogate the sapphire thin-film sensors has a low spectral density, the blackbody radiation at high temperatures induces a background spectrum to the total measured spectrum. In order to obtain the

reflection spectrum from the thin-film sensor only, two measurements were taken with the same settings on the spectrometer to cancel the spectrum by the blackbody radiation, as is described by Eq. (3):

$$
\begin{aligned}
I_1(\lambda) &= I_n(\lambda) + I_{bbr}(\lambda)I_2(\lambda) \\
&= I_n(\lambda) + I_{bbr}(\lambda) + I_h(\lambda) \cdot I_{sp}(\lambda) \\
&\quad \cdot [I_{DC} + I_{AC} \cdot \cos(2\pi OPD/\lambda - \varphi_0)].
\end{aligned}
\tag{3}
$$

$I_n(\lambda)$ denotes the dark noise equivalent spectrum of the spectrometer, and $I_{bbr}(\lambda)$ is the measured spectrum from the blackbody radiation. The halogen light source was turned off at the first measurement and turned on at the second measurement. The difference of the two measurements is only determined by the OPD of the thin-film sensor, assuming $I_h(\lambda)$ and $I_{sp}(\lambda)$ are known in advance. It is noticed that Eq. (3) assumes no other significant reflections in the optical link other than those from the thin film. This is generally a good approximation because the reflections from both thin film sides are much larger than other ones due to the big refractive index discontinuity on both sides of the thin film.

As temperature of the thin film changes, its OPD varies accordingly, thus the measured spectrum from the thin-film sensor shifts. Figure 6 presents the measured spectra at different temperatures, from which it is seen clearly that the fringes are shifting toward the longer wavelength as a result of an increased OPD when the temperature increases. It should be pointed out that since the halogen light source has a noisy spectrum, all measured spectra were smoothed first by averaging each detector pixel in the spectrometer with its 100 neighboring pixels in order to reduce the noise in the spectra, as shown in Fig. 6.

The ZrO$_2$ thin-film sensor was calibrated by the "wavelength-tracking" method [14]. The measured spectra, as shown in Fig. 6, have multiple visible peaks and valleys (labeled as A, B, C, D), which can be selected as key points for the wavelength-tracking algorithm. Each peak and valley was locally fitted to a parabolic curve for precise measurement of
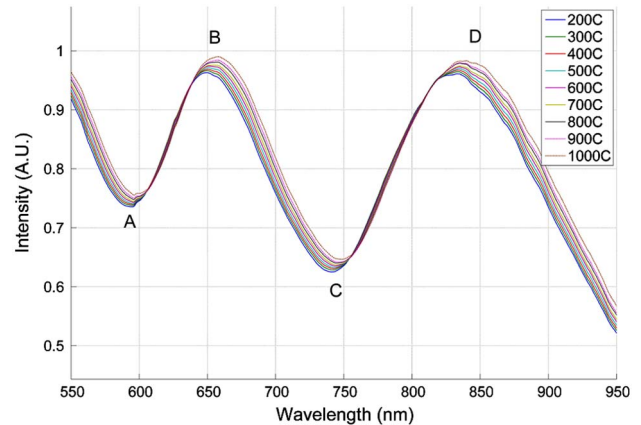

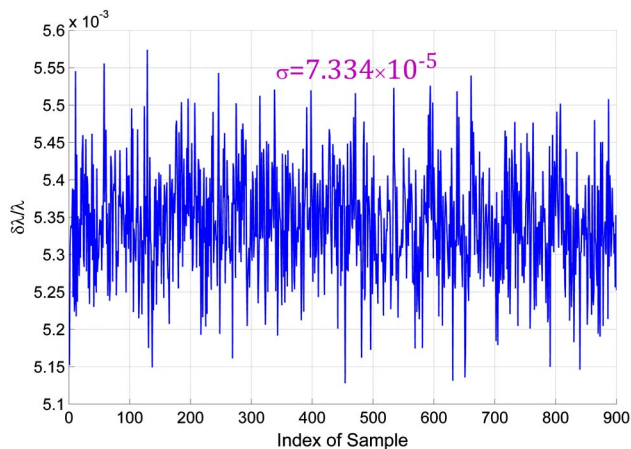Fig. 6. (Color online) Reflection spectra of a ZrO$_2$ thin-film sensor at different temperatures.

Fig. 7. (Color online) Relative wavelength shift of the ZrO_2 thin-film sensor measured at 1000 °C.

Fig. 8. (Color online) Calibration curve for the ZrO_2 thin-film sensor.

its location. As temperature changes, the relative wavelength shift $\Delta\lambda/\lambda$ can be calculated by continuously monitoring the peak or valley wavelength. According to Eq. (2), the relative wavelength shift $\Delta\lambda/\lambda$ depends only on the material properties of the ZrO_2 thin film, thus averaging across all available peaks and valleys can further improve the calibration accuracy.

The spectrometer used in this study has 3,648 pixels that cover a wavelength range from 347 nm to 1040 nm. The average wavelength separation per pixel is calculated to be 0.19 nm. The resolution of the peak-tracking measurement was quantified by monitoring the thin-film sensor at a constant temperature of 1000 °C, at which the identified relative wavelength shift $\Delta\lambda/\lambda$ had the largest fluctuation. A total of 900 samples were acquired during a one-hour test. The calculated relative wavelength shift had a one-sigma variation of 7.334×10^{-5} (Fig. 7).

The ZrO_2 thin-film sensor was then calibrated in a furnace (Thermolyne 48000), which was heated from 200° to 1000 °C. The wavelength-tracking method was used to monitor and record the relative wavelength shift for each of the available peaks and valleys, and reference temperature measurements were taken using a K-type thermocouple. The values of the relative wavelength shift $\Delta\lambda/\lambda$ were averaged to obtain a more accurate calibration curve (Fig. 8). A third-order polynomial curve was fitted to the data to obtain a full-scale sensor calibration.

As is seen from the calibration curve, the relative wavelength shift is found to be 1.009×10^{-2} over an 800 °C temperature span, thus the sensitivity is calculated to be

$$S = \frac{\Delta\lambda}{\lambda \cdot \Delta T} = \frac{1.009 \times 10^{-2}}{800\,°C} = 1.262 \times 10^{-5}/°C. \quad (4)$$

The one-sigma resolution of the relative wavelength shift at 1000 °C is 7.334×10^{-5} (Fig. 7), the equivalent one-sigma temperature resolution of the ZrO_2 thin-film sensor is calculated to be 5.8 °C, using
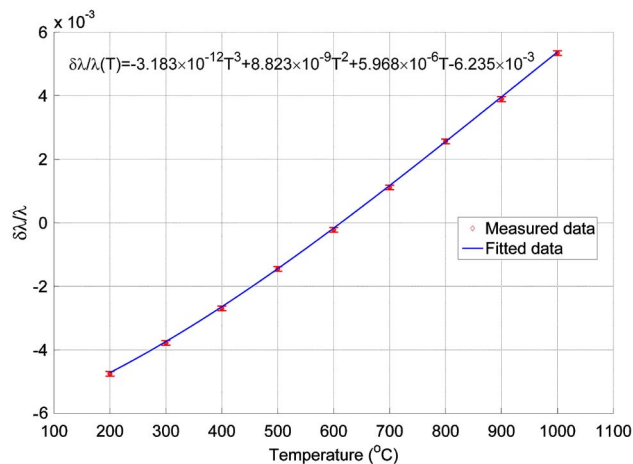
the sensitivity calculated from Eq. (4). The resolution is generally good enough for most high-temperature applications. The low-temperature resolution of the thin-film sensor is mainly due to the poor wavelength resolution of the spectrometer, which can be improved by using a larger detector array in the spectrometer.

5. Conclusion

We have reported a ZrO_2 thin-film-based sapphire fiber high-temperature sensor. A submicrometer thick ZrO_2 thin film was coated on the polished tip of a sapphire fiber to form a Fabry-Perot interferometric sensor. Low-coherence interferometry was used to interrogate the ZrO_2 thin-film sensors with an estimated temperature resolution of 5.8 °C in the temperature range 200° to 1000 °C. Given the above results, it is believed that ZrO_2 is a good material candidate to fabricate miniaturized thin-film temperature sensors on sapphire fiber tips. This batch fabrication method is very attractive for mass sensor production.

References

1. G. N. Merberg and J. A. Harrington, "Optical and mechanical properties of single-crystal sapphire optical fibers," Appl. Opt. **32**, 3201–3209 (1993).
2. R. Dils, "High-temperature optical fiber thermometer," J. Appl. Phys. **54**, 1198–1201 (1983).
3. Y. Zhu, Z. Huang, F. Shen, and A. Wang, "Sapphire-fiber-based white-light interferometric sensor for high-temperature measurements," Opt. Lett. **30**, 711–713 (2005).
4. H. Xiao, J. Deng, G. Pickrell, R. G. May, and A. Wang, "Single-Crystal sapphire fiber-based strain sensor for high-temperature applications," J. Lightwave Technol. **21**, 2276–2283 (2003).
5. J. Wang, B. Dong, E. Lally, J. Gong, M. Han, and A. Wang, "Multiplexed high temperature sensing with sapphire fiber air gap-based extrinsic Fabry-Perot interferometers," Opt. Lett. **35**, 619–621 (2010).
6. D. Grobnic, S. J. Mihailov, C. W. Smelser, and H. Ding, "Sapphire fiber Bragg grating sensor made using femtosecond

laser radiation for ultrahigh temperature applications," IEEE Photon. Technol. Lett. **16**, 2505–2507 (2010).

7. J. Wang, E. Lally, B. Dong, J. Gong, and A. Wang, "Fabrication of a miniaturized thin-film temperature sensor on a sapphire fiber tip," IEEE Sens. J. **11**, 3406–3408 (2011).

8. G. Tilloca, "Thermal stabilization of aluminium titanate and properties of aluminium titanate solid solutions," J. Mater. Sci. **26**, 2809–2814 (1991).

9. Y. S. Touloukian, R. K. Kirby, R. E. Taylor, and T. Y. R. Lee, *Thermophysical Properties of Matter*, Vol. **13**: Thermal Expansion Nonmetallic Solids (IFI/Plenum, 1977).

10. M. A. Clevinger, *Phase Diagrams for Ceramists. Bibliographic update through January 1, 1989, and cumulative indexes for volumes I–VIII* (American Ceramic Society, 1990).

11. C. J. Howard, R. J. Hill, and B. E. Reichert, "Structures of ZrO_2 polymorphs at room temperature by high-resolution neutron powder diffraction," Acta Crystallogr. Sect. B **44**, 116–120 (1988).

12. M. Bocanegra-Bernal and S. Díaz De La Torre, "Phase transitions in zirconium dioxide and related materials for high performance engineering ceramics," J. Mater. Sci. **37**, 4947–4971 (2002).

13. Y. Zhu and A. Wang, "Surface-mount sapphire interferometric temperature sensor," Appl. Opt. **45**, 6071–6076 (2006).

14. B. Qi, G. Pickrell, J. Xu, P. Zhang, Y. Hong, W. Peng, Z. Huang, W. Huo, H. Xiao, R. G. May, and A. Wang, "Novel data processing techniques for dispersive white light interferometer," Opt. Eng. **42**, 3165–3171 (2003).